17

Tide Gauge Observations of the Indian Ocean Tsunami December 26, 2004, at the Río de la Plata Estuary, Argentina

Walter Dragani, Enrique D'Onofrio, Dernis Mediavilla
Walter Grismeyer and Mónica Fiore
Servicio de Hidrografía Naval and UBA/CONICET
Argentina

1. Introduction

The Río de la Plata (RDP), located on the eastern coast of southern South America at approximately 35°S (Fig. 1), is one of the largest estuaries of the world (Shiklomanov, 1998). It has a northwest to southeast oriented funnel shape approximately 300 km long that narrows from 220 km at its mouth to 40 km at its upper end (Balay, 1961). The estuarine area is 35,000 km^2 and the fluvial drainage area is 3.1 x 10^6 km^2. The system drains the waters of the Paraná and Uruguay rivers, which constitutes the second largest basin of South America. Therefore, it has a large discharge with a mean of around 25,000 m^3 s^{-1}, and maximum values as high as 50,000 m^3 s^{-1} under extreme conditions (Jaime et al., 2002). The RDP can be divided into three regions: upper, with an averaged depth of less than 3–5 m, intermediate, 5–8 m deep, characterized by the presence of several shallow sand banks and an outer region with depths ranging from 10 to 20 m (Dragani & Romero, 2004). Throughout its system of dredged channels the RDP estuary constitutes the main maritime access to Argentina and Uruguay.

Water level stations located along the estuary constitute a tide gauge network with the main purpose of recording water level heights associated not only with tides but also with the atmospheric forcing which produces storm surges (D'Onofrio et al., 1999). Tides in the RDP present a mixed, primarily-semidiurnal regime. Tides have a spring range of 1.58 m at Santa Teresita (Argentina) and 0.38 m at Punta del Este (Uruguay) located on the Atlantic coast, at the south-western and north-eastern side of the RDP mouth, respectively. The tidal range increases north-westward: 0.72 m at Punta Indio Channel, 1.01 m at La Plata and 1.10 m at Buenos Aires (Fig. 2), along the RDP southern coast. On the other hand, along the Uruguayan coast, the tidal range varies: 0.68 m at Montevideo, 0.66 m at Colonia del Sacramento (known as Colonia) and 0.76 m at Martín García Island (SHN, 2010). The coincidence of large or even moderate high tides and large meteorologically induced surges has historically caused catastrophic floods in many coastal areas of the Buenos Aires Province (D'Onofrio et al., 1999).

Sea level oscillations in the frequency band from a few minutes to almost two hours have been frequently observed at different tide stations along the Buenos Aires coast (Balay, 1955; Inman et al., 1962; Dragani et al., 2002; Dragani et al., 2009). Dragani (1988) studied a

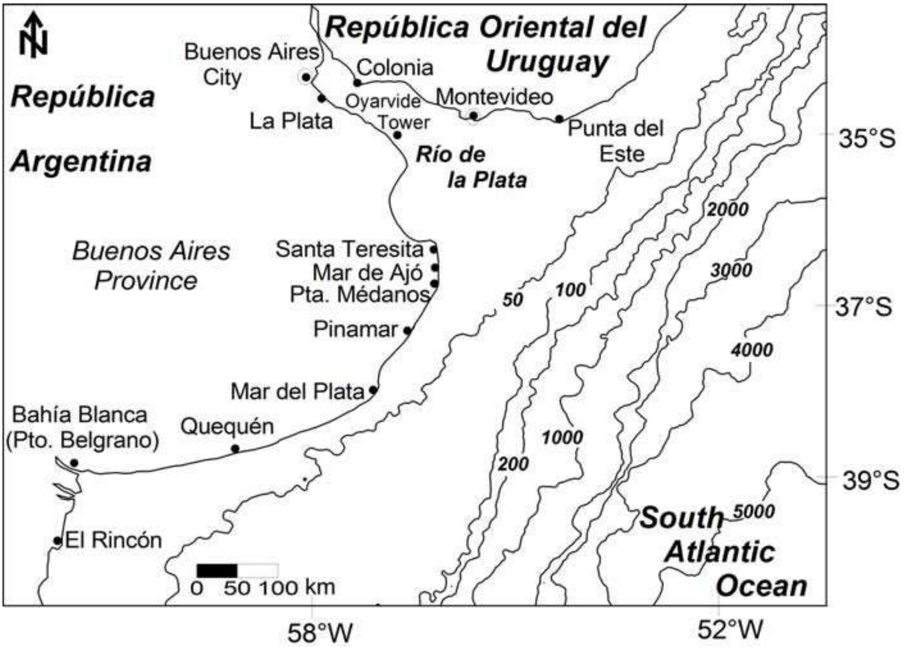

Fig. 1. Buenos Aires Province and Río de la Plata estuary. Bathymetry contours are in meters. Source: nautical charts SHN (1992, 1993)

possible relationship between oceanic seismic activity and energetic sea level oscillation events detected at Pinamar (Fig.1) but, due to the low correlation between both phenomena, it was suggested that a different mechanism would be required to generate these sea level oscillations. Dragani (1997) and Dragani et al. (2002) showed that, during high sea level activity, spectral peaks covered almost the whole frequency band between 1.1 and 4.7 cph (cycles per hour). Significant coherence values estimated between Mar de Ajó and Mar del Plata (172-km apart, Fig. 1) have clearly shown that this is a regional phenomenon. Based on the occurrence of simultaneous atmospheric gravity waves and long ocean wave events, the similarities of the spectral structures of both waving phenomena (Dragani et al., 2002) and the high effectiveness in the atmospheric-ocean energetic transference (proved by numerical simulations), it was possible to conclude that atmospheric gravity waves are the most probable forcing mechanism able to generate long ocean waves on the Buenos Aires continental shelf (Dragani, 2007). Dragani (1997) described the typical synoptic situation during sea level oscillation events in the coastal waters of the Buenos Aires province. Low level atmospheric cyclonic circulation and the passage of atmospheric fronts were always present prior to and during those events. Upper-air soundings obtained at Bahía Blanca (Fig. 1) meteorological station showed a lower pronounced tropospheric inversion that depicts an example of the state of the atmosphere when a frontal surface lies overhead. This tropospheric inversion constitutes an optimal interface for the propagation of high amplitude atmospheric gravity waves (Nuñez et al., 1998).

At 00:59 UTC on 26 December 2004, a moment magnitude (MW) 9.3 megathrust earthquake occurred along 1300 km of the oceanic subduction zone located 100 km west of Sumatra and

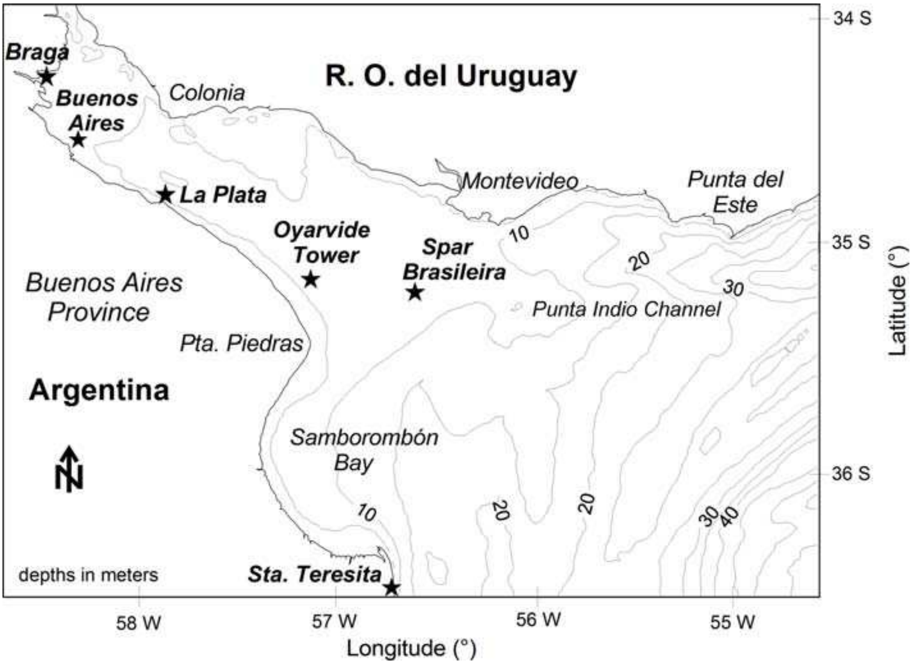

Fig. 2. Río de la Plata estuary. 5 m depth contours are depicted

the Nicobar and Andaman Island in the eastern Indian Ocean. The waves recorded around the world revealed unprecedented, truly global reach of the waves generated on December 26 (Titov et al., 2005). This tsunami is the first for which there are high-quality worldwide tide-gauge measurements. Tsunami amplitudes from many gauges along the Indian Ocean coast-line reached several meters and in some cases the waves were large enough to destroy the tide gauge recording equipment (Merrifield et al., 2005). All these records, together with those from other countries, demonstrate that this particular tsunami was a truly global event (Woodworth et al., 2005).

Filtered sea level oscillations recorded at Santa Teresita, Mar del Plata and Puerto Belgrano (Fig. 1) were studied by Dragani et al. (2006). At Mar del Plata, Santa Teresita and Puerto Belgrano, the Indian Ocean tsunami first arrived as a trough and the perturbations persisted approximately two days after the initial arrival. Initial waves were not the largest ones in the group. At Mar del Plata and Santa Teresita the largest waves were not observed until 7.8 and 17.8 hours after the first arrival, respectively. The first arrival detected was at Mar del Plata on December 27, 2004, at 00:15 UTC. At Santa Teresita and Puerto Belgrano, the tsunami reached the coast 33 minutes and 4.5 hours, respectively, after the arrival at Mar del Plata. Maximum wave height determined at Santa Teresita, Mar del Plata and Puerto Belgrano stations were 0.27, 0.15 and 0.20 m, respectively. Amplitudes and periods (ranging from 20 to 120 minutes) presented noticeable temporal variability while the oscillations persist. Oscillations lasted 40 hours at Mar del Plata and the perturbation was longer at Santa Teresita (54 hours). The mean (December 25 to 28 2004) sea level pressure field (NOAA-CIRES/Climate Diagnostics Center, www.cdc.noaa.gov) showed a low-pressure cell located east of the RDP estuary and a high-pressure cell located south of the low cell, at

50°S. During December 25 to 28 easterlies prevailed in the lower troposphere over the whole coastal area of Buenos Aires province. This weather pattern is completely different to the ones associated with frontal passages over the area. The tropospheric inversion necessary for the development of atmospheric gravity waves (capable of generating sea level oscillations in the region with periods similar to the tsunami waves) was not present in the RDP or in the adjacent continental shelf on December 25 to 28, 2004.

At the present, water level perturbations associated with the Indian oceanic tsunami have never been reported in the Río de la Plata estuary. Both tide gauges operating in the Río de la Plata estuary (at Buenos Aires and Oyarvide Tower stations), maintained by the Servicio de Hidrografía Naval (SHN) of Argentina, have a sampling interval of 60 minutes which is too long to resolve the signals corresponding to the tsunami. Recently, Jan de Nul (Hidrovía S.A. at Argentina), an international dredging company, provided several temporal high resolution water level data series positioned at different locations (Fig. 2) of the RDP. Consequently, it was possible to present the first description of the water level oscillations in the upper RDP associated to the tsunami generated as a response to the Sumatra earthquake. Even though these perturbations reached only 0.05 – 0.10 m, it was practically unthinkable that a tsunami wave would reach and propagate along the RDP before the Sumatra earthquake. In addition, a numerical experiment was performed to determine the vulnerability of the coast of the Buenos Aires Province to a hypothetical severe tsunami generated in the Mid Atlantic Ridge of the South Atlantic Ocean. The validation of this numerical model was carried out by comparing the maximum amplitudes simulated and the ones recorded at the selected tide stations located in the RDP , after the occurrence of the earthquake and subsequent tsunami in Sumatra (December 2004).

2. The Indian ocean tsunami, 2004, at the RDP. Observational study

Sea level records from a tide gauge located in the open sea (Santa Teresita) and from five tide gauges located along the RDP were analyzed. Pressure sensors were installed at Santa Teresita (ST: 36˚ 32' S, 56˚ 40' W), Spar Brasileira (SB: 35˚ 10′ S, 56˚ 37′ W), Oyarvide Tower (OT: 35˚ 06′ S, 57˚ 08′ W), La Plata (LP: 34˚ 50′ S, 57˚ 53′ W), Buenos Aires (BA: 34˚ 34′ S, 58˚ 23′ W) and Braga (BR: 34˚ 20′ S, 58˚ 29′ W) (Fig. 2). Out of all tide stations, ST is the only one exposed to the open sea, located about 20 km south of the RDP mouth (Figs. 1 and 2). SB is approximately in the middle of the imaginary line connecting Montevideo and Punta Piedras, which is the limit between the outer and intermediate RDP. OT is located in the intermediate RDP and LP, BA and BR stations were emplaced in the upper RDP. Except ST, the five tidal stations are disposed approximately 50-80 km apart, along the navigation channel access to the Buenos Aires Port (Argentina).

Water levels were measured by pressure transducers 312P TECMES (http://www.tecmes.com) which are commonly used to measure hydrostatic column height variations. Thermally compensated, the sensor is housed in a stainless steel capsule highly resistant to impacts. The system includes a vent tube for automatic compensation of the variations of the atmospheric pressure. Pressure sensors were fixed approximately 2 m below the tidal datum. The accuracy given by the pressure sensor is approximately ±0.1% of the instrument depth (±0.002 m). At SB, OT, LP, BA and BR these sensors were set with a data acquisition sampling interval of 20 min but, at ST, a lower sampling interval (6 min) was adopted. Sea level oscillations from December 26 12:00 to 29 00:00, 2004, (h = +3) recorded at ST, SB, OT, LP, BA and BR are shown in Fig. 3. It can be noted that the tide

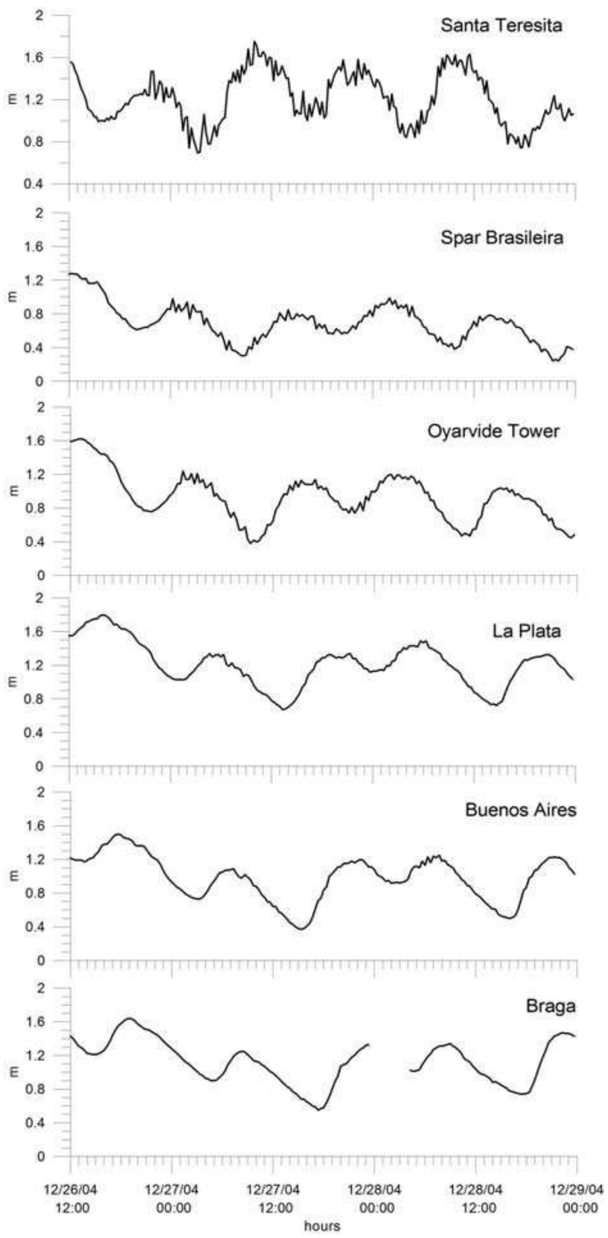

Fig. 3. Sea level records (m) at Santa Teresita, Spar Brasileira, Oyarvide Tower, La Plata, Buenos Aires and Braga. Time in hours from December 26, 2004, 12:00 (h = +3)

gauge at Braga did not work between 12/27 23:00 and 12/28 03:00. Sea level data contain diurnal and semidiurnal tides and higher-frequency oscillations ranging from a few minutes to two hours. Water level data were convoluted by means of Kaiser-Bessel bandpass filters

(201 elements), which select periods of approximately 12 - 180 minutes, and provide an attenuation factor of 100 dB outside that range (Hamming, 1977; Harris, 1978).
Filtered sea level oscillations at selected stations (Fig. 2) are shown in Fig. 4. At ST and LP the Indian Ocean tsunami first arrived as a trough and at SB, OT, BS and BR it arrived as a crest. The perturbations persisted approximately two days after the initial arrival. Initial waves were not the largest ones in the group. At ST, SB, OT, LP, BA and BR the largest waves were not observed until 7.8, 2.5, 7.6, 1.6, 23.3 and 23.0 h after the first arrival, respectively (Table 1). Arrival times were estimated by the first measured increase or decrease before the crest or trough. The first arrival detected was at ST on December 27, 2004, at 21:48. At SB and OT, the tsunami reached the gauge at 1.86 and 3.52 h, respectively, after the arrival at ST. The wave reached the locations of LP, BA and BR, in the upper RDP, at 6.52, 7.85 and 9.18 h, respectively, after the arrival at Santa Teresita. Consequently, the tsunami wave lasted approximately 9 h to propagate from the RDP mouth (ST) to the upper RDP (BR). Maximum wave height (distance from trough to crest or vice versa) determined at ST, SB, OT, LP, BA and BR were 0.27, 0.20, 0.13, 0.09, 0.08 and 0.05 m, respectively (Table 1). It can be clearly appreciated that maximum wave height decreases noticeably from the outer to the upper RDP. A possible explanation of this feature could be related to the shallowness of the RDP estuary. In the middle RDP, near to the Argentine coast, the mean depth is less than 5 m and, in the upper part of the estuary, the mean depth is less than 3 m (Fig.2). Consequently, tsunami waves could be significantly attenuated due to friction dissipation and refractive effects.
Amplitudes and periods presented noticeable temporal variability while the oscillations persisted. It was considered that the activity persisted as long as amplitudes in the filtered records were higher than two root mean square of the water level before the beginning of the activity. Then, it was estimated that the tsunami wave activity lasted approximately 40-50 h in the RDP estuary. The main characteristics of the recorded tsunami waves at ST, SB, OT, LP, BA and BR (arrival time, maximum wave height and approximate duration of the sea level activity) are summarized in Table 1. Lags in the time of first arrivals between consecutive tide stations were also calculated considering the tsunami wave speed along the imaginary line connecting gauges in the RDP. Distances between consecutive gauges from SB to BR (Fig. 2) are 50 km (SB – OT), 80 km (OT – LP), 60 km (LP – BA) and 35 km (BA – BR). Mean depth through each consecutive pair of stations were computed from nautical charts SHN (1999a; b).

Location	Arrival time (h= +3)	Max. height (m)	Duration (h)
ST	12/26 21:48	0.27	54.00
SB	12/26 23:40	0.20	44.33
OT	12/27 01:20	0.13	41.33
LP	12/27 04:20	0.09	59.33
BA	12/27 05:40	0.08	58.33
BR	12/27 07:00	0.05	36.00

Table 1. Arrival time (h = +3), maximum wave height (m) and duration of the activity (h) obtained from water level records gathered at Santa Teresita (ST), Spar Brasileira (SB), Oyarvide Tower (OT), La Plata (LP), Buenos Aires (BA) and Braga (BR)

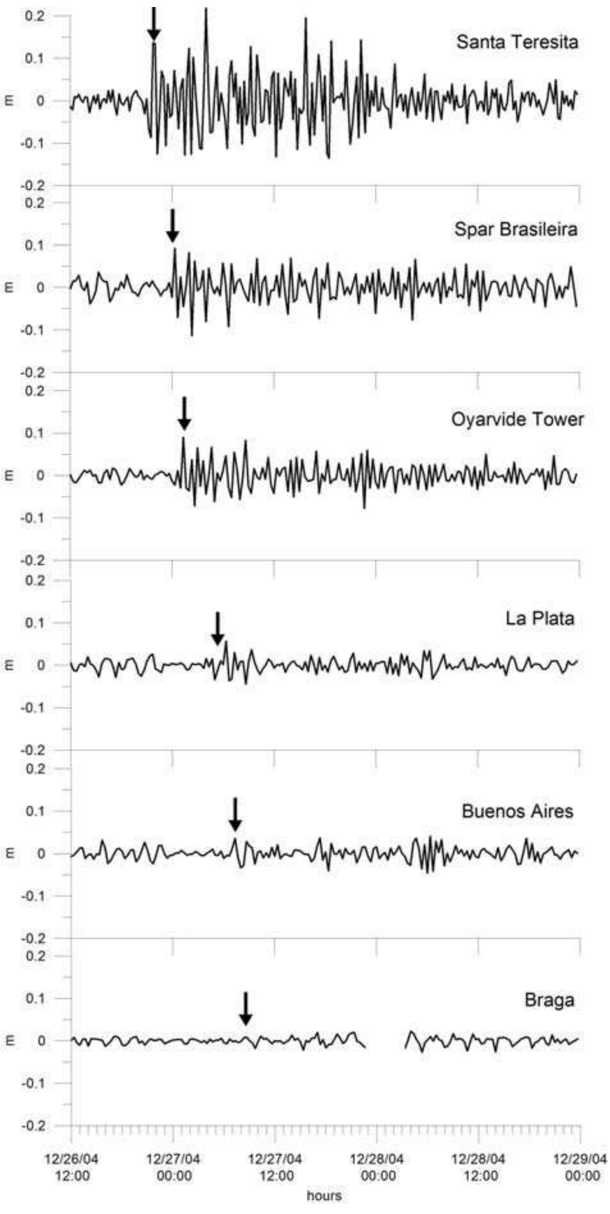

Fig. 4. Passband filtered sea level records (m) at Santa Teresita, Spar Brasileira, Oyarvide Tower, La Plata, Buenos Aires and Braga. Time in hours from December 26, 2004, 12:00 (h = +3). Arrows point out the beginning of the activity

The wave speed, c, of long ocean waves could be reasonably approximated by $(g\ h)^{1/2}$ (e.g., Dean & Dalrymple, 1984) where g is the acceleration due to gravity and h the local depth. According to the expression for c and using the corresponding distances and depths, the computed time lags between SB – OT, OT – LP, LP – BA and BA – BR resulted in 1.55, 2.65, 1.97 and 1.53 h, respectively, which match reasonably well with the observed times (1.66, 3.00, 1.33 and 1.33 h, respectively). It must be highlighted that depth variations produced by tide have not been included in this rough estimation of times. Computed and observed travel time, from SP to BR, resulted 7.70 and 7.32 h, respectively.

3. The Río de la Plata estuary: vulnerability to regional tsunamis

The southeastern coast of South America, and specially the RDP, has been traditionally considered to have low hazard probability of being affected by tsunamis. The main reason is the emplacement in a stable, tectonically inactive and passive continental margin (Mouzo, 1982; Urien & Zambrano, 1996). However, some geological, topographical and oceanographic aspects of the surrounding regions were reviewed as they could favor the occurrence of destructive events or contribute to increase damage. The Scotia Arc, located between the southernmost extreme of South America and the Antarctic Peninsula, is a highly dynamic convergent margin with frequent occurrence of earthquakes and volcanic eruptions (USGS-NEIC, 2008). The geographical positions of the strongest earthquakes in this region are pointed out in Fig. 5. Five relatively stronger earthquakes (magnitudes ≥ 7.5) have been recorded between 45°S – 65°S and 15°W – 75°W, nine earthquakes, with magnitudes ranging from 7.0 to 7.4, and ninety-two earthquakes, with magnitudes ranging from 6.0 to 6.9, have been recorded in this region. These earthquakes present the highest spatial density of hypocenters around the South Sandwich Islands, located at the eastern extreme of the Scotia Arc.

Considering the regional geotectonic setting, the configuration and the relative geographical position of Argentine coasts, the vulnerability to long ocean waves originated by submarine events like earthquakes, volcanic eruptions and slides in the Scotia Arc and surroundings was numerically studied by Dragani et al. (2008). The smooth and gently sloping continental shelf (Parker et al., 1997) is a feature that can behave as a "ramp" for ocean waves approaching the coast driven by either climatic or geological processes. The variable shelf width (decreasing from 600 to 170 km from South to North) and the morphology of the adjacent continental slope were considered as probable factors affecting the propagation of ocean waves. Regarding coastal morphology, there is an alternation of areas with different susceptibility to damaging effects coming from processes and events originated in the ocean. Results obtained from numerical simulations (Dragani et al., 2008) showed that bathymetric refraction is highly significant on the continental shelf producing a considerable divergence of energy which attenuates the long ocean wave amplitudes on the Patagonian coast (between 45° and 55°S). Maximum amplification factors were obtained at Southern Malvinas and Burdwood bank because the wave propagates almost without refracting and the transformation by shoaling is highly significant. Based on these preliminary numerical simulations, it was concluded that the Argentinean coast, and specially the RDP estuary, present a relatively low vulnerability to the tsunami wave generated by earthquakes whose epicenters are located at Scotia Arc. On the other hand, it is evident that tectonism, magmatism, volcanism and submarine slides at different settings of the Mid Atlantic Ridge in the South Atlantic Ocean must be seriously taken into account when evaluating the possibility of generation of ocean waves affecting the RDP. But, no strong submarine earthquakes, between 20°S and 50°S, have been reported in this region. Furthermore, no evidence of paleotsunamis have been mentioned for the Argentine coasts and marine

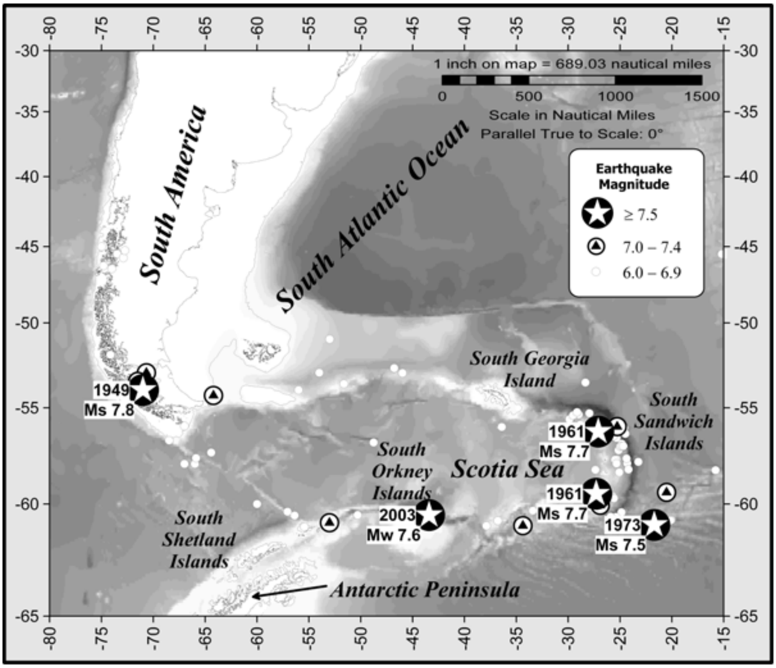

Fig. 5. Southwestern Atlantic Ocean and Antarctic Peninsula region. Locations of earthquakes which occurred in this area are pointed out with white stars, black triangles or white circles for earthquakes whose magnitudes were equal or higher than 7.5, ranged from 7.0 to 7.4 or from 6.0 to 6.9, respectively. Source: USGS-NEIC (2008)

geological records. However, the potential hazard of the RDP region should not be disregarded. Consequently, the amplification and propagation of a tsunami wave produced by a hypothetical strong earthquake in the South Atlantic Ocean will be analyzed by means of a validated numerical model.

4. Numerical simulations and numerical experiments

The model used for the numerical investigations is WQMap version 5.0 (Water Quality Mapping), developed by Applied Science Associates Inc. (ASA, 2004). The mathematical description of sea levels and currents requires the simultaneous solution of the dynamic equations of motion and the continuity equation. It is assumed that vertical accelerations are negligible, pressures are hydrostatic over depth and fluid density is homogeneous. The bottom stress is parameterized by means of a quadratic law in terms of the depth averaged current velocity and a constant value equal to 0.002 was selected for the non dimensional drag or bottom friction coefficient. Transient floor perturbations vertically forcing the ocean water column, like those produced during submarine earthquakes can not be included as forcing in WQMap model. In other words, this model is not able to generate surface sea level oscillation produced by earthquakes whose epicenters are located in the computational domain. The tsunami wave (when it is far enough from the epicenter) can be considered as a long wave (wavelength is longer than hundreds of kilometers) propagating in the ocean like

a shallow water wave (Dean and Dalrymple, 1984). WQMap model resulted to be a very efficient tool (Dragani et al., 2008) to simulate the propagation of this kind of waves on the Buenos Aires and Patagonian continental shelf waters (Fig. 5).
A realistic tsunami wave perturbation was imposed as boundary condition in the eastern border of the implemented computational domain (31°S to 45°S and 44°W to 66°W), between the RDP and the hypothetic epicenter of the earthquake. Sea level perturbations along selected grid points of the eastern open boundary were defined by means of a simple sinusoidal expression. Sea level oscillated only during three periods at every grid point of the open boundary, representing the incoming of the tsunami wave to the computational domain. The original bathymetry was obtained from an assemblage of nautical charts published by the Servicio de Hidrografía Naval of Argentina (SHN, 1992 and 1993), for the continental shelf (depths lower than 200 m) and a 1'x1' resolution depth data set coming from GEBCO (2003) for the continental slope and deep ocean. A square inverse distance method was used to create a regularly spaced grid from irregularly spaced bathymetry data. The resulting bathymetry was taken at 6.2 km x 5 km intervals, thus there are 281 grid points in the east-west and 312 grid points in the north-south directions. This grid represents a rectangular domain with a distance of 1,924 km in the east-west and 1,560 km in the north-south directions. The resulting grid has the shallowest depths (1.2 m) in the upper estuary and the greatest depths (deeper than 5,000 m) at the south-eastern corner of the domain. The adopted time step was 5 minutes. A set of experiments (Dragani, 2008) was designed to simulate the propagation characteristics of the tsunami wave from the deep ocean (boundary, 44°W meridian) to the coast and the best result was obtained for wave amplitude equal to 0.03 m and period 1 h.
Observed bandpass filtered water level (Fig. 4) and simulated water level oscillations (Fig. 6) are compared. Simulated maximum wave height at ST, SB, OT, LP and BA resulted 0.22, 0.13, 0.09, 0.07 and 0.05 m, respectively, and, although they are a little underestimated, they are in reasonable good agreement with the measurements (Table 2). Simulated lags between initial activity times corresponding to consecutives locations were also computed and presented in Table 3. Simulated water level at Braga was discarded from these comparisons because the modeled maximum wave height resulted extremely low, under 0.02 m. Similarly to the observed filtered records (Fig. 4) the largest simulated heights were observed after the first arrival of the wave. Perhaps, the main difference between observed and simulated water levels is the larger activity period corresponding to the observations. A possible explanation of this difference could be that the spatial resolution of the model is not enough to represent the complex geometry of the natural sand banks and channels in the RDP.

Location	Observed max. height (m)	Simulated max. height (m)
ST	0.27	0.22
SB	0.20	0.13
OT	0.13	0.09
LP	0.09	0.07
BA	0.08	0.05
BR	0.05	< 0.02

Table 2. Observed and simulated maximum wave height (m) at Santa Teresita (ST), Spar Brasileira (SB), Oyarvide Tower (OT), La Plata (LP), Buenos Aires (BA) and Braga (BR)

Consecutive stations	Observed lag (h)	Simulated lag (h)	Theoretic lag (h)
SB – OT	1.66	1.50	1.55
OT – LP	3.00	2.66	2.65
LP – BA	1.33	1.50	1.97

Table 3. Observed, simulated and theoretical lags (h) between consecutive tidal stations, from Spar Brasileira to Braga

It was shown that maximum amplitudes recorded at the RDP (after the occurrence of earthquake and subsequent tsunami occurred on December 26, 2004 in Sumatra) were realistically simulated using WQMap model. This validated model was used to study the potential vulnerability in the RDP to a hypothetical severe tsunami occurred in the Mid Atlantic Ridge of the South Atlantic Ocean.
The afore described numerical experiment was replayed, but a simple sinusoidal wave of 0.5 m amplitude (instead of 0.03 m) was imposed as forcing at the eastern boundary of the computational domain. Simulated water levels at ST, SB, OT and BA are presented in Fig. 7. LP and BR are not included in this figure because the simulated water levels resulted very similar to the ones of BA.

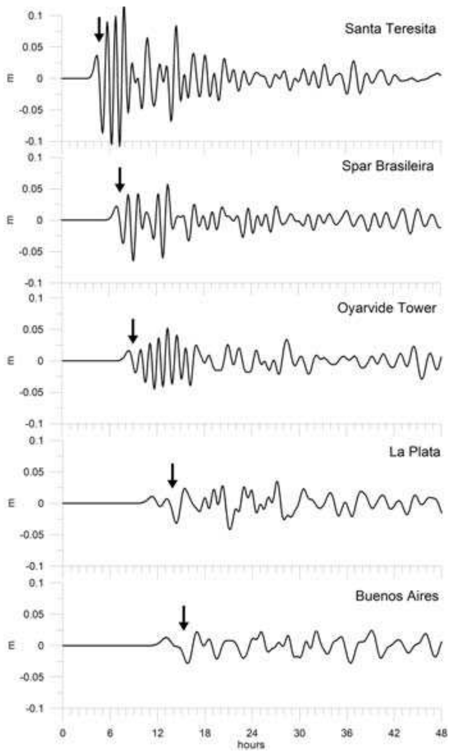

Fig. 6. Simulated sea level oscillation (m) at Santa Teresita, Spar Brasileira, Oyarvide Tower, La Plata and Buenos Aires, forced with wave amplitude equal to 0.03 m at the eastern boundary. Arrows point out the beginning of the activity

Maximum wave height determined at ST, SB, OT and BA were 3.25, 1.10, 0.70 and 0.25 m, respectively. It can be clearly appreciate that maximum wave height decreases drastically from ST to BA. This simulation shows that shallow water effects (especially refraction and bottom friction) could play a very significant roll in the propagation and transformation of the tsunami wave from the outer to the upper RDP. Maximum wave height decreased 13 times from the RDP mouth (ST: 3.25 m) to the upper RDP (BA: 0.25 m) and 3-4 times from the RDP mouth to the outer and intermediate RDP. Therefore, it can be concluded that Buenos Aires City and the coast at the upper RDP, where millions of inhabitants are settled, present very low vulnerability to tsunamis generated by earthquakes with epicenters located at the Mid Atlantic Ridge of the South Atlantic Ocean.

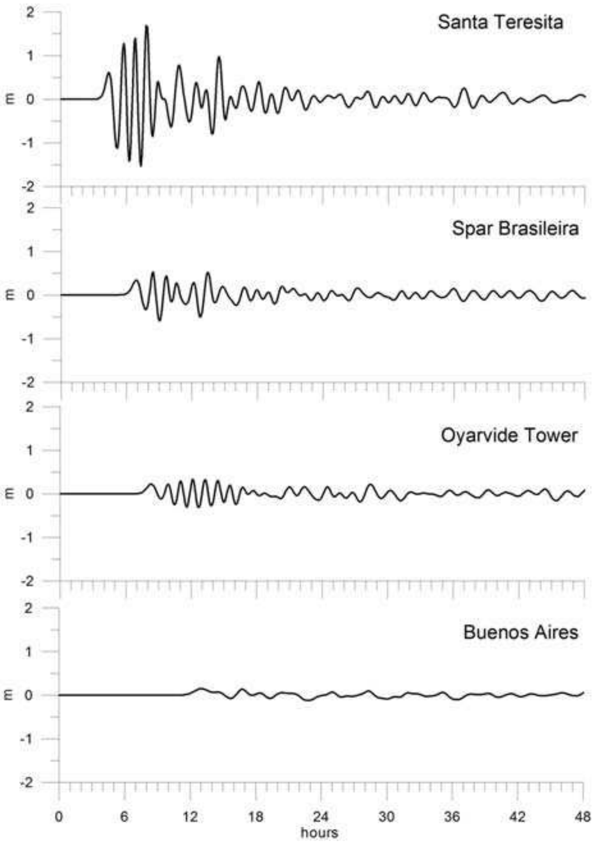

Fig. 7. Simulated sea level oscillation (m) at Santa Teresita, Spar Brasileira, Oyarvide Tower and Buenos Aires, forced with wave amplitude equal to 0.50 m at the eastern boundary

On the contrary, Samborombón bay presents relatively high vulnerability to this kind of natural hazards. This bay is located 160 km southeast of the city of Buenos Aires (Fig. 2) and receives the Samborombón River from the northwest and the Salado River from the west, as well as several canals draining the bay's low, irrigated hinterland, which is part of the humid Pampa, an extensive area of fertile plains. Samborombón bay was established as

Ramsar site 885 (01/24/1997) in response to Article 2.1 of the Convention on Wetlands (Ramsar, Iran, 1971, www.ramsar.org). A very high amount of organisms of the intertidal zone of the southernmost part of the bay are predated every summer by a high number of migratory birds that use Bahía Samborombón as a refuel station. The whole bay is characterized by soft bottoms of fine sediments with high percentage of mud and organic matter and very low slope beach. Maximum wave heights ranged from 3.25 m (at ST, 20 km southward the southern limit of the bay) to 1.10 - 0.70 m (at SB and OT, respectively, located at the northernmost part of the bay) could flood a very significant coastal area, especially, if a severe tsunami wave reached these low coasts during spring high water and/or during storm surge conditions.

5. Conclusions

The south-eastern coast of South America, and specially the RDP, has been traditionally considered to have low hazard probabilities of being affected by tsunamis. At 00:59 UTC on 26 December 2004, a moment magnitude (MW) 9.3 megathrust earthquake occurred in the eastern Indian Ocean generating a wave tsunami measured in almost all the World Ocean demonstrating that this particular wave was a truly global event (Woodworth et al., 2005). Even though this perturbation reached only a few centimeters high at the upper RDP, before the occurrence of the Sumatra earthquake, the propagation of a tsunami wave along the RDP was unthinkable. Water level records from a tide gauge located at the open sea and from five tide gauges located along the RDP were analyzed and discussed in this work. Water level oscillations at selected stations persisted approximately two days after the initial arrival of the tsunami. Initial waves were not the largest ones in the group. Maximum wave height determined at Santa Teresita, Spar Brasileira, Oyarvide Tower, La Plata, Buenos Aires and Braga (Fig. 2) were 0.27, 0.20, 0.13, 0.09, 0.08 and 0.05 m, respectively showing that maximum wave height decreased noticeably from the outer to the upper RDP. A possible explanation of this feature could be related to the shallowness of the RDP estuary, where the tsunami wave heights could be significantly attenuated due to friction dissipation and refractive effects.

Even though, no strong submarine earthquakes, between 20°S and 50°S, have been reported in this region of the ocean, the vulnerability of the RDP to a tsunami wave produced by a hypothetic strong earthquake in the South Atlantic Ocean was numerically studied by means of a validated model. The model used for this investigation was WQMap (version 5.0). Simulated water level oscillations were slightly underestimated but they were in good agreement with the observations (Fig. 4, Fig. 6 and Table 2). Similarly to the observed filtered records (Fig. 4) the largest simulated heights were produced after the first arrival of the wave. The main difference between observed and simulated water levels was the longer duration of the observed events. This difference could be attributed to the relatively low spatial resolution of the model domain, which might have not been enough to represent the complex geometry of the natural sand banks and channels at the RDP. This validated model was used to carry out a numerical experiment in which a hypothetical strong tsunami propagated from the Mid Atlantic Ridge in the South Atlantic Ocean to the upper RDP. The numerical experiment, using a simple sinusoidal wave of 0.5 m amplitude, showed that the maximum wave height decreased 13 times from the RDP mouth (ST: 3.25 m) to the upper RDP (BA: 0.25 m) indicating that shallow water transformation (especially refraction and bottom friction) could play a very significant role in the propagation of the tsunami wave from the outer to the upper RDP. Consequently, it could be preliminarily concluded that the Buenos Aires City and the coast along the upper RDP, would present very low vulnerability to tsunamis generated by earthquakes whose epicenters were located in the South Atlantic Ocean. On the contrary, Samborombón bay (Fig. 2) shows a relatively higher vulnerability to this kind of natural hazards because it has a very low slope beach and the simulations showed that the maximum wave height ranged from 3.25 m to 1.10 - 0.70 m, between the southernmost and northernmost extremes of the bay. It is evident that this hazardousness could be greater if a severe tsunami wave reached this low coast during spring high water and/or during a storm surge conditions.

6. References

ASA (2004). Applied Science Associates. WQMap User Manual, Version 5.0. Applied Science Associates Inc, Narraganset, RI, USA.

Balay, M. (1955). La determinación del nivel medio del Mar Argentino, influencias de las oscilaciones del mar no causadas por la marea, Dir. Gral. de Nav. Hidrog., Min. de Marina, pp. 46.

Balay, M.A. (1961). El Río de la Plata entre la atmósfera y el mar, Publ. H-621, 153 pp., Serv. de Hidrogr. Nav. Armada Argentina, Buenos Aires.

Dean, R.G. & Dalrymple, R.A. (1984). Water wave mechanics for Engineers and scientistics, Prentice-Hall, Englewood Cliffs, New Jersey, pp. 353.

D'Onofrio, E. E.; Fiore, M. M. E. & Romero, S. I. (1999). Return periods of extreme water levels estimated for some vunerable areas of Buenos Aires, Continental Shelf Research, 19, 1681-1693.

Dragani, W.C. (1988). Análisis del proceso físico generador de ondas largas en la costa bonaerense argentina, Thesis, Inst. Tec. Bs. As., Buenos Aires, pp. 65.

Dragani, W.C. (1997). Una explicación del proceso físico generador de ondas de largo período en la costa bonaerense argentina, Doctoral Thesis, Facultad de Ciencias Exactas y Naturales, Universidad de Buenos Aires, pp. 222.

Dragani, W.C.; Mazio, C. A. & Nuñez, M. N. (2002). Sea level oscillations in coastal waters of the Buenos Aires Province, Argentina, Continental Shelf Research, 22, 779-790.

Dragani, W.C. & Romero, S. I. (2004). Impact of a possible local wind change on the wave climate in the upper Río de la Plata. International Journal of Climatology, 24(9), 1149-1157.

Dragani, W. C.; D'Onofrio, E.E.; Grismeyer W. & Fiore M.E. (2006). Tide gauge observations of the Indian Ocean tsunami, December 26, 2004, in Buenos Aires coastal waters, Argentina. Continental Shelf Research 26, 1543-1550.

Dragani, W. C. (2007). Numerical experiments of the generation of long ocean waves in coastal waters of the Buenos Aires Province, Argentina, Continental Shelf Research. doi:10.1016/j.csr.2006.11.009.

Dragani, W.C.; D'Onofrio, E.E.; Grismeyer, W.; Fiore, M.E.; Violante, R. & Rovere, E. (2008). Vulnerability of the Atlantic Patagonian coast to tsunamis generated by submarine earthquakes located in the Scotia Arc region. Some numerical experiments. Natural Hazards, doi:10.1007/s11069-008-9289-4.

Dragani, W.C.; D'Onofrio, E.E.; Grismeyer, W.; Fiore, M. & Campos, M. I. (2009). Atmospherically-induced water oscillations detected in the Port of Quequén, Buenos Aires, Argentina. Journal of Physics and Chemistry of the Earth 34 998–1008.

GEBCO (2003). User guide to the centenary edition of the GEBCO Digital Atlas and its data sets. Ed. M. T. Jones, Natural Environment Research Council.

Hamming, R. W. (1977). Digital filters, Prentice Hall, Signal Processing Series, pp. 221.

Harris, F. J. (1978). Of the use of windows for harmonics analysis with the discrete Fourier Transform, Proc. IEEE, 66, 51-83.

Inman, D.; Munk, W. & Balay, M. (1962). Spectra of low frequency ocean waves along the Argentine shelf, Deep-Sea Res., 8, 155-164.

Jaime, P.; Menéndez, A.; Uriburu Quirno, M. & Torchio, J. (2002). Análisis del régimen hidrológico de los ríos Paraná y Uruguay, Informe LHA 05-216-02, 140 pp., Inst. Nac. del Agua, Buenos Aires.

Merrifield, M. A.; Firing, Y. L.; Aarup, T.; Agricole, W.; Brundrit, G.; Chang-Seng, D.; Farre, R.; Kilonsky, B.; Knight, W.; Kong, L.; Magori, C.; Manurung, P.; McCreery, C.; Mitchell, W.; Pillay, S.; Schindele, F.; Shillington, F.; Testut, L.; Wijeratne, E.M.S.; Caldwell, P.; Jardin, J.; Nakahara, S.; Porter, F.Y. & Turetsky, N. (2005). Tide gauge observations of the Indian Ocean tsunami, December 26, 2004, Geophysical Research Letter, 32, LO9603, doi:10.1029/2005GL022610.

Mouzo, F.H. (1982). Geología Marítima y Fluvial. In: Historia Marítima Argentina, Armada Argentina. Cuántica Editora, Buenos Aires, Tomo I, Secc. 2: 117.

Nuñez, M.N.; Mazio, C.A. & Dragani, W. C. (1998). Estudio espectral de un lapso de intensa actividad de ondas de gravedad atmosféricas registradas en la costa bonaerense argentina, Meteorológica, 23, (1 and 2), 47-54.

Parker, G.; Paterlini, C.M. & Violante, R.A. (1997). El Fondo Marino. In: El Mar Argentino y sus Recursos Pesqueros (E.E. Boschi, Ed.), INIDEP, Mar del Plata, Argentina. 1: 65-87.

SHN (1992). Nautical Chart H-1: Acceso al Río de la Plata, Serv. Hidrog. Nav., Buenos Aires.

SHN (1993). Nautical Chart H-2: El Rincón, Golfos San Matías y Nuevo, Serv. Hidrog. Nav., Buenos Aires.

SHN (1999a). Nautical Chart H-113: Rio de la Plata Exterior, Serv. Hidrog. Nav., Buenos Aires.

SHN (1999b). Nautical Chart H-116: Rio de la Plata Médio y Superior, Serv. Hidrog. Nav., Buenos Aires.

SHN (2010). Tablas de Marea, H-610, Serv. Hidrog. Nav., Buenos Aires.

Shiklomanov, I. A. (1998). A summary of the monograph world water resources: A new appraisal and assessment for the 21st Century, report, U. N. Environ. Programme, Nairobi.

Titov, V.; Rabinovich, A.B.; Mofjeld, H.O.; Thomson, R.E. & González, F.I. (2005). The global reach of the 26 December 2004 Sumatra tsunami, Science, 309, 2045-2048.

Urien, C.M. & Zambrano, J.J. (1996). Estructura de la Plataforma continental, in "Geología y Recursos Naturales de la Plataforma Continental Argentina" (V.A. Ramos and M.A. Turic, eds.). Relatorio XIII Congreso Geológico Argentino y III Congreso de

Exploración de Hidrocarburos, Asociación Geológica Argentina-Instituto Argentino del Petróleo, Buenos Aires: 29-65.
USGS-NEIC (2008). United States Geological Survey - National Earthquake Information Center, http://earthquake.usgs.gov/regional/neic/
Woodworth, P.L.; Blackman, D.L.; Foden, P.; Holgate, S.; Horsburgh, K.; Knight, P.J.; Smith, D.E.; Macleod, E.A. & Bradshaw, E. (2005). Evidence for the Indonesian Tsunami in British tidal records, Weather, 60, 9, 263-267.

The Tsunami Threat - Research and Technology
Edited by Nils-Axel MÃ¶rner

ISBN 978-953-307-552-5
Hard cover, 714 pages
Publisher InTech
Published online 29, January, 2011
Published in print edition January, 2011

Submarine earthquakes, submarine slides and impacts may set large water volumes in motion characterized by very long wavelengths and a very high speed of lateral displacement, when reaching shallower water the wave breaks in over land - often with disastrous effects. This natural phenomenon is known as a tsunami event. By December 26, 2004, an event in the Indian Ocean, this word suddenly became known to the public. The effects were indeed disastrous and 227,898 people were killed. Tsunami events are a natural part of the Earth's geophysical system. There have been numerous events in the past and they will continue to be a threat to humanity; even more so today, when the coastal zone is occupied by so much more human activity and many more people. Therefore, tsunamis pose a very serious threat to humanity. The only way for us to face this threat is by increased knowledge so that we can meet future events by efficient warning systems and aid organizations. This book offers extensive and new information on tsunamis; their origin, history, effects, monitoring, hazards assessment and proposed handling with respect to precaution. Only through knowledge do we know how to behave in a wise manner. This book should be a well of tsunami knowledge for a long time, we hope.

InTech Europe
University Campus STeP Ri
Slavka Krautzeka 83/A
51000 Rijeka, Croatia
Phone: +385 (51) 770 447
Fax: +385 (51) 686 166
www.intechopen.com

InTech China
Unit 405, Office Block, Hotel Equatorial Shanghai
No.65, Yan An Road (West), Shanghai, 200040, China
中国上海市延安西路65号上海国际贵都大饭店办公楼405单元
Phone: +86-21-62489820
Fax: +86-21-62489821